Computer Simulation of the Surface Free Energy of the Si(100) Surface and the Line Free Energies Associated with Steps on This Surface†

Sweta Somasi and Bamin Khomami

Department of Chemical Engineering, Washington University, St. Louis, Missouri 63130

Ronald Lovett*

Department of Chemistry, Washington University, St. Louis, Missouri 63130

Received: May 26, 2004; In Final Form: August 14, 2004

Many atomic-level 0 K thermodynamic properties of silicon (100) surfaces have been calculated from classical potential energy surfaces or from quantum ground-state Born−Oppenheimer surfaces. We present an easy and accurate computer simulation method for determining surface thermodynamic properties at high temperatures where the dynamics may be described classically. The method is illustrated with calculations of the surface free energies of the 2×1 and $c(2 \times 2)$ reconstructed (100) surfaces at $T = 1000$ K using the Stillinger−Weber interaction model for silicon. We then use an extension of our simulation method to determine the line free energies associated with steps. Enough examples of line free energies are given to enable us to calculate the equilibrium concentration of single and double steps as a function of the surface miscut angle. We also deduce the activation free energy associated with the Si adatom hopping over simple steps.

I. Introduction

The silicon (100) surface is the most commonly used substrate for making electronic devices. Considerable effort has been directed toward estimating surface properties theoretically, because it is very difficult to measure thermodynamic properties of solid surfaces in the laboratory. Most estimates (minimum potential energy computations or quantum mechanical ground-state energy calculations) give properties at temperature $T = 0$ K. But crystals are typically grown at $T \approx 1000$ K, and it is natural to suppose that there are significant entropic contributions to surface properties at these temperatures. In this paper, we illustrate how computer simulations can be used to determine thermodynamic properties of silicon surfaces at $T > 0$ K .

Stillinger and Weber[1] (SW) developed a semiempirical potential to describe the bulk properties of silicon. As this potential also gives a good description of the reconstructions that take place on Si(100) surfaces,[2] we have used this potential in our simulations. The structures of the 2×1 and $c(2 \times 2)$ reconstructions are reviewed in Section II. Our simulation method for determining surface free energies is described in Section III along with our SW-based calculations of the surface free energies of the 2×1 and $c(2 \times 2)$ reconstructed surfaces at $T = 1000$ K.

In practice, cutting a crystal to produce a nominal (100) surface actually produces a high-index surface with a surface free energy greatly in excess of that of a perfect (100) surface. At equilibrium, these surfaces rearrange into (100)-oriented strips separated by steps. The simplest step structures are reviewed in Section IV. It is a minor extension of our surface free energy calculation to determine the line free energy associated with these steps. The extension is described in Section V along with numerical results for a handful of simple steps. We use these results to determine the equilibrium distribution between single and double steps.

† Part of the special issue "Frank H. Stillinger Festschrift".

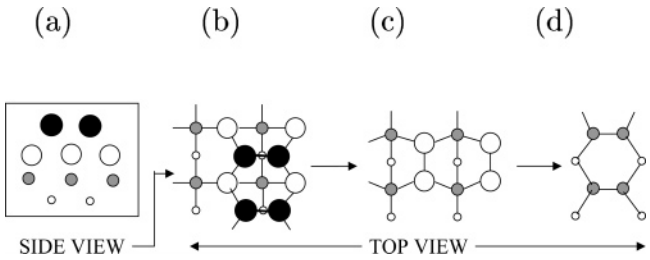

Figure 1. The four top layers of atoms at a (100) surface are shown in (b). The black circles represent the atoms in the top layer, as keyed in (a). While the atoms on the surface dimerize, those in the lower layers remain on essentially square lattices. The orientation of the dimers, however, is determined by the structure of the second layer. In (c), the top layer of (b) has been removed, and the new surface layer dimerizes in the opposite direction. Removing one more layer gives (d).

Even at 1000 K, the motion of adatoms on a Si(100) surface is too slow to observe in a computer simulation. Nevertheless, we can determine the activation free energy of specific hops[3] and, hence, estimate the rate at which these hops will occur. The results for the most important hops over steps are given in Section VI. Finally, in Section VII, we compare our surface simulation method with previously used methods, and we review the assumptions we have made in modeling silicon surfaces.

II. The Structure of the Silicon (100) Surface

The atoms in a (100) plane inside a bulk crystal are arranged on a square lattice. The lattices on adjacent planes are staggered with a periodicity of four planes. At a free surface, one-half of the Si−Si bonds are missing, and the surface reconstructs to form parallel dimers[4] with the dimer direction determined by the structure of the (100) plane beneath the surface (see Figure 1). There are many ways to place parallel dimers on a square lattice, however. Consecutive dimers can be arranged in the

10.1021/jp047713e CCC: $27.50
Published on Web 11/04/2004

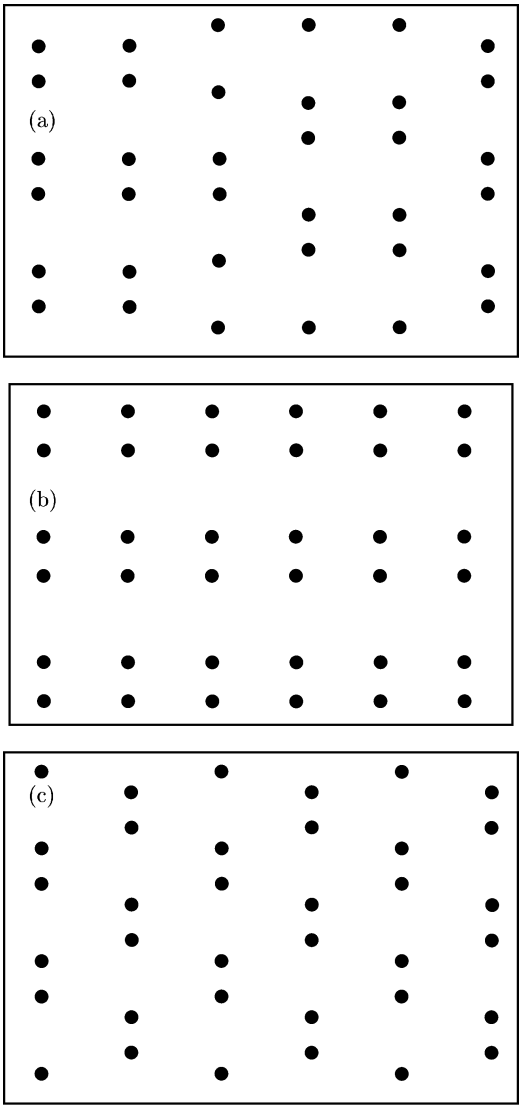

Figure 2. (a) shows the configuration of the surface atoms on a (100) surface that was created in a noisy environment. A rough mixture of 2 × 1 and $c(2 \times 2)$ reconstructions can be seen. Pure 2 × 1 and $c(2 \times 2)$ reconstructions are shown in (b) and (c).

same row (a 2 × 1 reconstruction, Figure 2b) or in alternating rows (a $c(2 \times 2)$ reconstruction, Figure 2c), for example. Theoretical calculations[5,6] show that the 2 × 1 reconstruction has the lowest energy, and this is the reconstruction most often observed[7−9] at high temperatures. But other structures (e. g., a $c(2 \times 4)$ structure[8,10] at $T < 200$ K and a $c(4 \times 4)$ structure[11,12] in $600 < T < 750$ K) have been seen.

III. Calculation of Surface Free Energies

III.A. Simulating the Gibbs Subtractive Procedure. Let $A(T, N, V)$ denote the Helmholtz free energy of a real, finite system. Gibbs identified surface contributions to the free energy by expanding $A(T, N, V)$ asymptotically in $V^{-1/3}$. First, the free energy per unit volume

$$a(T,\rho) = \lim_{\substack{N\to\infty \\ V\to\infty \\ N/V\to\rho}} \left[\frac{A(T, N, V)}{V}\right] \qquad (1)$$

is identified. Then, the surface free energy γ is identified[2,5,6] as that part of the difference between $Va(T, N/V)$ and $A(T, N, V)$ that is proportional to the number of surface atoms N_s

$$\gamma = \lim_{\substack{N\to\infty \\ V\to\infty \\ N/V\to\rho}} \left[\frac{A(T, N, V, N_s) - Va(T, N/V)}{N_s}\right] \qquad (2)$$

It is difficult to realize this asymptotic expansion in the laboratory and even more difficult in a simulation. We can realize a system with complete translational invariance in a simulation, however, by imposing periodic boundary conditions. We identify $a(T, N/V)$ with the corresponding $A(T, N, V)/V$.

If the periodicity is removed in one direction, we create two surfaces separated by the period. If the original period was large enough that the middle of the crystal is bulklike, that the two surfaces are thermodynamically independent, we can take $[A(T, N, V, N_s) - Va(T, N/V)]/2N_s$ to be γ.

While we could take $a(T, N/V)$ from a simulation of a completely periodic system and $A(T, N, V, N_s)$ from another simulation of a system that is only periodic in two directions, the small contribution of γ to the difference means that the statistical uncertainty[13] in γ would be large. If, however, we construct a thermodynamic path on which the periodicity is removed in one direction, then (1) the free energy change on this path is precisely the free energy difference we want. The conjugate force we observe is always proportional to the surface area, so (2) we avoid taking the difference between two large numbers. Because the structural change on this path is small, (3) the statistical noise on this path is minimized, and accurate γ values are obtained.

In a molecular dynamics (MD) simulation, the equations of motion of a collection of atoms are solved numerically. For an N-atom system, the equations of motion are prescribed by giving the Hamiltonian

$$H = \sum_{i=1}^{N} \frac{\mathbf{p}_i^2}{2m} + V_N(\mathbf{r}_1, ..., \mathbf{r}_N) \qquad (3)$$

Stillinger and Weber construct $V_N(\mathbf{r}_1, ..., \mathbf{r}_N)$ from two and three body components as follows:

$$V_N(\mathbf{r}_1, ..., \mathbf{r}_N) = \sum_{1\le i<j\le N} V_2(\mathbf{r}_{ij}) + \sum_{1\le i<j<k\le N} V_3(\mathbf{r}_i,\mathbf{r}_j,\mathbf{r}_k) \qquad (4)$$

Our MD implementation differs from the dynamics of real systems in several ways: (1) The continuous motion in time is replaced by a sequence of discrete time steps. (2) Real boundaries are avoided by replicating the configuration of the N atoms in the basic cell, $0 \le x \le L_x$, $0 \le y \le L_y$, $0 \le z \le L_z$, periodically in all directions and including the interactions with all of the atoms in these images. (3) The N atoms are coupled to an additional coordinate, in the manner proposed by Nosé,[14] so that the distribution on the $\mathbf{r}_1, ..., \mathbf{r}_N$ is canonical, rather than microcanonical. The temperature T enters as a parameter in the equations of motion for the added coordinate. Our implementation of the Nosé scheme is described in Appendix A of ref 13. (4) The range of the SW potential is finite, so any given atom interacts with only a finite number of neighboring atoms.

III.B. A Practical Realization. In a determination[15] of the surface free energies of various surfaces of Lennard-Jones solids, we noted that the simplest implementation of the path suggested in Section III.A encounters a singularity. The singularity is easily avoided by using a two-step path. If this two-step path were followed with silicon, however, the nature of the reconstruction that would be realized is unpredictable. The final surface would be a mixture of possible stable and metastable reconstructions (as in Figure 2a, for example). As we want to learn the surface

free energies of specific reconstructions, we must force the system to adopt the reconstructions we seek. To do this, we replace the naive path of Section III.A with a three-step path.

III.B.1. Create a Surface in a Bulk Crystal without Changing the Crystal Structure. Step 1: In the first step, we remove one of the periodic boundary conditions. Let **T**(**B**) denote the atoms in the top (bottom) layers (i.e., in the surface layers just below the $z = L_z$ plane (above the $z = 0$ plane)) that interact with (images of) atoms on the opposite sides of these planes. The set **T**(**B**) is finite because of the finite range of the potential.

We wish to remove the interactions across the $z = L_z$ boundary to create a free surface. These are the interactions

$$V_{\text{surface}} = \sum_{i\in\mathbf{T},\, j\in\mathbf{B}} V_2(r_{ij}) + \sum_{i,j\in\mathbf{T},\, k\in\mathbf{B}} V_3(\mathbf{r}_i,\mathbf{r}_j,\mathbf{r}_k) + \sum_{i\in\mathbf{T},j,k\in\mathbf{B}} V_3(\mathbf{r}_i,\mathbf{r}_j,\mathbf{r}_k) \quad (5)$$

Removing the terms in V_{surface} creates two free surfaces. The remaining "bulk" interactions

$$V_{\text{bulk}} = V_N(\mathbf{r}_1, ..., \mathbf{r}_N) - V_{\text{surface}} \quad (6)$$

remain unaltered after the two surfaces have been created. In terms of these new symbols,

$$H = \sum_{i=1}^{N} \frac{\mathbf{p}_i^2}{2m} + V_{\text{bulk}} + V_{\text{surface}} \quad (7)$$

Substituting

$$V_{\text{surface}} \rightarrow \lambda V_{\text{surface}} + (1-\lambda)\sum_{i\in\mathbf{T}} U_i(\mathbf{r}_i) + (1-\lambda)\sum_{j\in\mathbf{B}} U_j(\mathbf{r}_j) \quad (8)$$

in eq 7 gives an $H(\lambda)$ that defines a thermodynamic path on which the interatomic forces across the $z = L_z$ plane are removed. When $\lambda = 1$, the system is fully periodic in all directions. When $\lambda = 0$, the interatomic interactions are those of a solid with two surfaces in external fields $\{U_j(\mathbf{r}_j)\}$ that are chosen to keep the surface atoms from moving off their original lattice sites. On this path (for each λ), the general relation

$$A'(\lambda) = \langle H'(\lambda)\rangle \quad (9)$$

reduces to

$$A_1'(\lambda) = \langle V_{\text{surface}} - \sum_{i\in T} U_i(\mathbf{r}_i) - \sum_{j\in T} U_j(\mathbf{r}_j)\rangle \quad (10)$$

$A_1'(\lambda)$ is the ensemble average of a mechanical quantity in a system with Hamiltonian $H(\lambda)$. We evaluate this as a time average.

If the surfaces became absolutely free, the surface would expand into the surrounding space. When $\lambda \rightarrow 0$, the two- and three-body interactions that prevent atoms on opposite sides of the $z = L_z$ surface from overlapping (the system remains periodic) are removed. The external fields $\{U_j(\mathbf{r}_j)\}$ prevent this overlap by standing in for the periodic interactions that are being removed. These fields also influence the magnitude of the fluctuations associated with $A_1'(\lambda)$. In fact, the effect of fluctuations is minimized by minimizing the change in the one-particle distribution function $\rho(\mathbf{r},\lambda)$ along the path.[16] Because the one-particle distribution about lattice sites in the bulk crystal is very close to a Gaussian distribution[13] with width $\Sigma = 0.011$ nm, the change in $\rho(\mathbf{r},\lambda)$ is minimized by binding a surface atom to the bulk lattice site $\mathbf{R}_{Bi}$ with the harmonic potential

$$U_i(\mathbf{r}_i) = \frac{1}{2}\kappa(\mathbf{r}_i - \mathbf{R}_{Bi})^2 \quad (11)$$

if

$$\kappa = k_B T/\Sigma^2 \quad (12)$$

III.B.2. Use the External Fields to Create the Desired Reconstruction. Step 2: At the end of Step 1, $\lambda = 0$, and all the properties of the system are independent of L_z. We may take $L_z \rightarrow \infty$ without doing any work. The system is a crystal with two surfaces but in the presence of an external field that preserves the bulk structure. We next use these external fields to move the surface atoms into the configuration of the targeted reconstruction.

The substitution

$$\sum_{i\in\mathbf{T}\cup\mathbf{B}} \frac{1}{2}\kappa(\mathbf{r}_i - \mathbf{R}_{Bi})^2 \rightarrow \sum_{i\in\mathbf{T}\cup\mathbf{B}} \frac{1}{2}\kappa(\mathbf{r}_i - \mathbf{R}_i(\eta))^2 \quad (13)$$

where

$$\mathbf{R}_i(\eta) = \mathbf{R}_{Bi} + \eta\cdot(\mathbf{R}_{Si} - \mathbf{R}_{Bi}) \quad (14)$$

and $\mathbf{R}_{Si}$ are the positions of the surface atoms after reconstruction, defines a path, parametrized by $\eta = 0 \rightarrow 1$, on which the surface is reconstructed. If $A_2(\mu)$ is the free energy on this path, then eq 13 gives

$$A_2'(\eta) = \langle\kappa[\mathbf{r}_i - \mathbf{R}_i(\eta)](\mathbf{R}_{Si} - \mathbf{R}_{Bi})\rangle_\eta \quad (15)$$

III.B.3. Relax the Surface Structure. Step 3: At the end of Step 2, $\eta = 1$, and the system has two surfaces in the presence of an external field. It remains to remove $U(\mathbf{r})$ to produce a system with two free surfaces. The substitution

$$\sum_{i\in\mathbf{T}\cup\mathbf{B}} U_i(\mathbf{r}_i) \rightarrow \mu \sum_{i\in\mathbf{T}\cup\mathbf{B}} U_i(\mathbf{r}_i) \quad (16)$$

defines a path, parametrized by μ, on which $U(\mathbf{r})$ is removed. If $A_3(\mu)$ is the free energy on this path,

$$A_3'(\mu) = \langle \sum_{i\in\mathbf{T}\cup\mathbf{B}} U_i(\mathbf{r}_i)\rangle \quad (17)$$

The net effect of these three steps is the creation of two free surfaces with the desired reconstructed surface. Thus,

$$\Delta A = 2N_s\gamma = \int_1^0 d\lambda\, A_1'(\lambda) + \int_0^1 d\eta\, A_2'(\eta) + \int_1^0 d\mu\, A_3'(\mu) \quad (18)$$

Figure 3 shows a sketch of the three calculational steps used to determine the surface free energy.

III.B.4. Numerical Results. We have used this three-step path to determine the surface free energies at $T = 1006$ K of the 2×1 and $c(2 \times 2)$ reconstructions shown in Figure 2b,c. Both reconstructions are stable on the simulation time scale. The bulk third law free energy of a silicon crystal was also calculated using the technique in ref 16 and was found to be 4.5466 ± 0.0015 eV/atom. This solid would be in equilibrium with a vapor of density $\rho_{\text{vap}} = 6.65 \times 10^{-20}$ moles/cm^3, so the interactions between atoms in the vapor phase and the solid make a negligible contribution to the surface free energies. No sublimation is seen during the simulation.

There were 432 atoms in the original crystals, and the final free 2×1 surfaces contained 36 atoms arranged in 3 dimer rows of 6 dimers each. The parameters used to define the

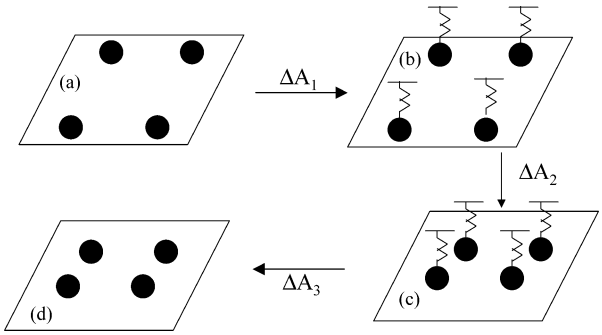

Figure 3. A drawing illustrating the three steps of the thermodynamic path used to calculate the surface free energy of a reconstructed surface.

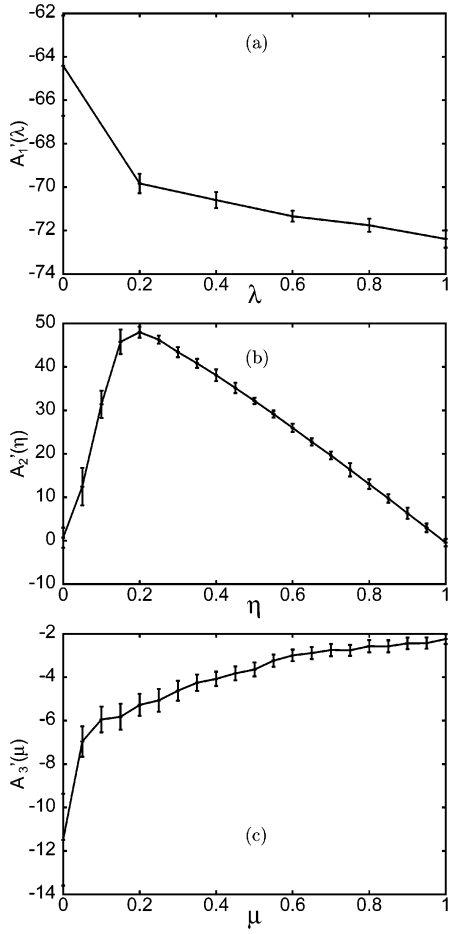

Figure 4. Contributions of the three steps to the surface free energy. (a) $A_1'(\lambda)$, (b) $A_2'(\eta)$, and (c) $A_3'(\mu)'$ for the 2×1 reconstruction along with the statistical uncertainty (the error bars) in the simulations for a crystal with 432 atoms, the top (bottom) surface having 36 (36) atoms.

reduced SW units are $\epsilon = 2.17$ eV, $\sigma = 0.209\,51$ nm, $m = 4.6457 \times 10^{-23}$ g, and $\tau = 7.66 \times 10^{-14}$ s. The step size in the simulations was 0.002 τ, the equilibration times were 10−20 τ, and the sampling times were 20−40 τ. The integrands in eq 18 were fit to a discrete set of simulated values: $\lambda, \eta, \mu = 0.00, 0.05, ..., 1.0$. We show $A_1'(\lambda)$, $A_2'(\eta)$, and $A_3'(\mu)$ for the 2×1 reconstruction in Figure 4.

The error bars shown in Figure 4 are the variances in the A''s observed in the simulations. The thermodynamically expected values for these variances is a measure of the thermodynamic stability of the intermediate states on the three steps. The variances are small, because these states are stable. The numerical values for the variances also include errors due to finite observation times and errors associated with incomplete equilibration. The surface free energies for the two reconstructions are given in Table 1 along with (column 3) the errors deduced from the variances shown in Figure 4 and (column 6) the 0 K surface energy results.[2]

TABLE 1: Surface Free Energy for Two 36-Atom Surfaces

surface	ΔA	$\sigma(\Delta A)$[a]	γ (SW units)	γ (eV)	γ (0 K)[2]
2×1	40.6979	0.61	0.565/atom	1.226	1.416
$c(2 \times 2)$	42.8168	0.23	0.595/atom	1.291	1.491

[a] The uncertainty in ΔA deduced from the observed variances in the thermodynamic forces on the integration paths.

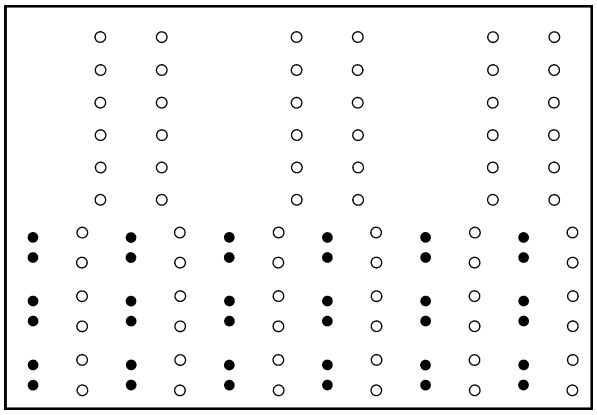

Figure 5. Configuration at an S_A step, using the shading pattern of Figure 1.

IV. Steps

There has been a lot of research on the nature of steps on Si(100) surfaces and the distribution of steps as a function of miscut angle, both experimentally[17−27] and computationally.[28−34] However, the inclusion of finite temperature effects has been very approximate at best.

Chadi[33] used S and D to denote single linear (one layer) and double (two layers) steps. He added the subscripts A and B to indicate the direction of the dimer rows in the upper terrace, A referring to a step oriented parallel to the dimers (as in Figure 5) and B to a step oriented perpendicular to the dimers (as in Figure 6). Because the direction of the dimer rows formed by consecutive (100) planes alternates (see Figure 1), an S_A step must be followed by an S_B step, etc. If the dimers in the lower terrace are oriented perpendicular to the direction of the step, it is possible to have a row of atoms that have no adjacent atoms with which to dimerize (Figure 6b). This is referred to as a "nonbonded" step. If this is not the case (Figure 6a), the step is referred to as "rebonded". The structure of the D_B step is shown in Figure 7. A D_A step will follow a D_A step, and a D_B step will follow a D_B step.

V. Calculation of Line Free Energies

If a crystal has N_{s1} atoms at one type of surface and N_{s2} atoms at another type, and N_e is the length of the step between the surfaces, we expect that

$$A(T, N, V, N_{s1}, N_{s2}, N_e) \approx Va(T, N/V) + N_{s1}\gamma_1 + N_{s2}\gamma_2 + N_e \beta \quad (19)$$

with β the free energy per atom associated with the edge. The extension of Gibbs' subtractive procedure would be

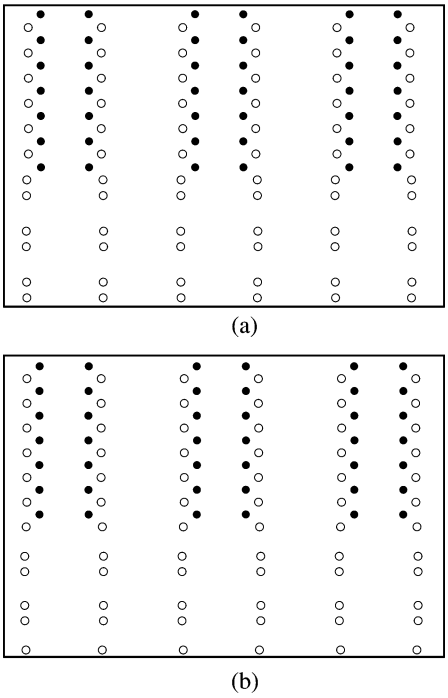

Figure 6. (a) Rebonded single step S_B and (b) Nonbonded single step S_B, using the shading pattern of Figure 1.

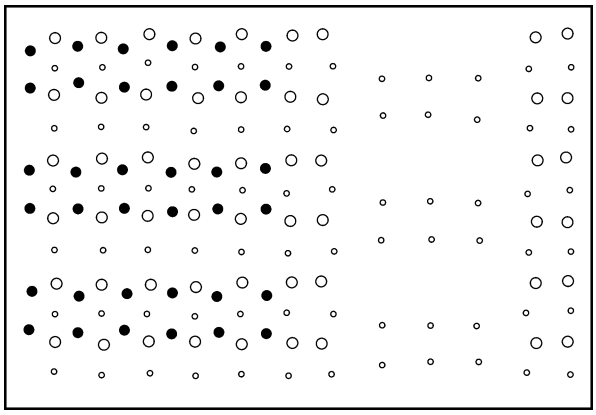

Figure 7. Configuration at a D_B step, using the shading pattern of Figure 1.

$$\beta = \lim_{\substack{N\to\infty \\ V\to\infty \\ N/V\to\rho}} \left[\frac{A(T, N, V, N_{s1}, N_{s2}, N_e) - Va(T, N/V) - N_{s1}\gamma_1 - N_{s2}\gamma_2}{N_e}\right] \quad (20)$$

We can estimate β associated with a step with a minor extension of the method used to calculate line free energies in Section III. The only change is that we start with a different crystal shape. Instead of starting with a regular parallelepiped crystal, we start with a crystal with a step (see Figure 8). When the system has periodic images in all three directions, the system is still pure bulk with no surface or step present. When periodicity is removed, two stepped surfaces are created. The free energy change ΔA calculated by the method of Section III now includes an additional contribution associated with the steps. If the nonstepped surface free energy is already known, the contribution of the added steps can be deduced from eq 20.

The step on the bottom surface is the complement of the step on the top surface, so an S_A step on the top surface is associated with an S_B step on the bottom surface. Thus, the total free energy change associated with the thermodynamic path introduced in Section III will be twice the surface free energy plus the line free energies associated with both S_A and S_B steps. At the end of Step 1, however, the configuration of the system is still that of the original bulk crystal. ΔA_1 can thus be divided equally between the two surfaces. In the subsequent steps, the free energy changes at the top and bottom surfaces can be easily distinguished. Thus, we can separately determine β_{SA} and β_{SB}. For the double steps, the same step is present on both surfaces.

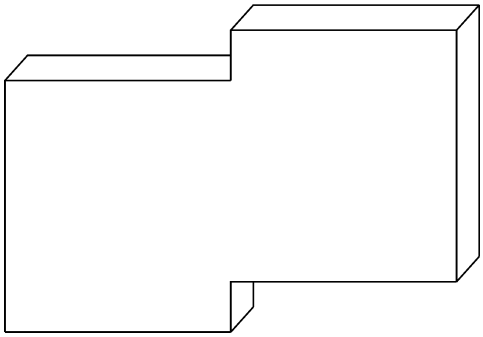

Figure 8. Crystal shape used to calculate line free energies.

TABLE 2: Line Free Energies (eV/atom at Edge)

step	crystal	rebonded
S_A	$12 \times 6 \times 12$	0.07
S_B	$14 \times 6 \times 16$	0.33
D_A	$12 \times 6 \times 12$	0.73
D_B	$14 \times 6 \times 16$	0.30

Our numerical results are shown in Table 2. The S_A step has a much lower line free energy than the other steps, because it is the step with the least structural mismatch across the step. Because of our choice of period in the direction perpendicular to the D_A surface, our D_A configuration was not completely rebonded (despite the column label). As this step is not seen experimentally, we did not try to distinguish rebonded and nonbonded configurations.

Numerically,

$$\beta_{D_B} < \beta_{S_A} + \beta_{S_B} \quad (21)$$

This agrees with the ordering of the energy estimates[33] and suggests that S_A and S_B steps would coalesce into D_B steps. In our simulations, we guide the reconstruction of the surface so that the step appears at a predetermined place and the steps do not move during our simulations. There are, however, many possible positions for the step, so our calculations really give a standard free energy β°. The complete free energy also contains a step concentration dependent term[29,30] that forces all double steps to dissociate if the total concentration of steps is low. Only single steps are seen experimentally at small miscut angles. At larger angles, only double steps are seen.[17,19,20]

We can quantify this approximately. If we assume that the concentrations of steps are sufficiently low that the real surface is an ideal mixture of steps, then the chemical potential of the steps will have an ideal form. If there were l_D double steps on a surface of extent $L \times$ the (100) lattice constant ($2\sqrt{2/3} \times$ the bond length), then

$$\mu_D = \beta^\circ_{D_B} + k_B T \ln \frac{l_D}{L} \quad (22)$$

is the rate at which the free energy changes with l_D. If there were l_S pairs of single steps, then

$$\mu_S = \beta^\circ_{S_A} + \beta^\circ_{S_B} + 2k_B T \ln \frac{2l_S}{L} \tag{23}$$

is the rate at which the free energy changes with l_S. Equilibrium between the number of single and double steps requires

$$K_{eq} = \exp(\beta^\circ_{D_B} - \beta^\circ_{S_A} - \beta^\circ_{S_B})/k_B T = \frac{4l_S^2}{Ll_D} \tag{24}$$

With the numbers in Table 2, $K_{eq} = 0.316$.

Because the rise per double step is $2/\sqrt{3} \times$ the bond length, the average miscut angle ϕ of a surface with steps is determined by

$$\tan \phi = \frac{l_D + l_S}{\sqrt{2}L} \tag{25}$$

Equations 24 and 25 fix the number of steps in terms of K_{eq} and ϕ. For example,

$$\frac{l_S}{L} = \frac{K_{eq}}{8}\left(\sqrt{1 + \frac{16\sqrt{2}\tan\phi}{K_{eq}}} - 1\right) \tag{26}$$

The transition between single and double step dominated surfaces occurs at the angle for which $l_D = l_S$. This is fixed by

$$\tan \phi = \frac{K_{eq}}{2\sqrt{2}} = 0.1117 \tag{27}$$

which gives $\phi = 6.4°$.

VI. The Rate of Adatom Hopping Over Steps

A silicon surface has a variety of silicon adatom binding sites (i.e., sites where a silicon atom is localized for a sufficiently long time that a binding free energy may be associated with the site). We have previously located the binding sites and determined the binding free energies for the simple 2×1 (100) surface.[3] Similar sites are present near a step, and it is important to know how the rate of hopping over a step compares with the rate of hopping across a flat surface.

While adatom hopping is too slow to be seen in a simulation of a 1000 K system, we can nevertheless simulate all of the properties required by transition-state theory to predict the hopping rates. Essentially, we must determine the heights of the free energy barriers associated with the various hopping paths.

Only states with lifetimes that are longer than local equilibration times have a free energy, so the description in terms of free energy barriers is only jargon. At an atomic level, hops occur infrequently because of the paucity in an equilibrium ensemble of mechanical trajectories connecting different sites. If we use a density of states in phase space to measure the variation of the number of states along a reaction path, this density must become very small somewhere along the path. The density of states is a geometrical property of phase space that does have an equilibrium expectation, however. If $\mathcal{D}$ is some region in phase space between binding sites, the probability of finding a system in $\mathcal{D}$ is

$$\text{prob} = \int\int_{\mathcal{D}} dp\, dq\, e^{-\beta H(p,q)} / \int\int dp\, dq\, e^{-\beta H(p,q)} \tag{28}$$

But we can characterize a region $\mathcal{D}$ by (invoking density functional theory) giving a potential $U(\mathbf{r})$ that confines the adatom to $\mathcal{D}$. With this characterization, eq 28 is equivalent to

$$\text{prob} = \int\int dp\, dq\, e^{-\beta[H(p,q)+U]} / \int\int dp\, dq\, e^{-\beta H(p,q)} = e^{-\beta\{A[U]-A[0]\}} \tag{29}$$

By identifying the phase integrals thermodynamically, this probability is related to the difference between the free energy of a system in the field $U(\mathbf{r})$, $A[U]$, and the free energy of a field-free system, $A[0]$.

Although we are interested in domains $\mathcal{D}$'s that are too improbable to see, we can still measure $A[U] - A[0]$ by constructing a path that connects the two states and measuring the conjugate force along the path as was done in Sections III and V. The hopping problem presents two new features, however. First, we do not actually know what the reaction coordinate is. The location of the adatom itself, for example, has the same velocity distribution as all of the other atoms in the system. It is not the slowly evolving coordinate required for transition-state theory to apply. The actual reaction coordinate is some collective motion of the adatom and substrate atoms. Rather than try to identify the reaction coordinate, however, we introduce a control variable into $U(\mathbf{r})$. If hopping occurred in one dimension, for example, the potential

$$U(x) = \frac{1}{2}k(x - X)^2 \tag{30}$$

biases the adatom configurations so that $\langle x \rangle \approx$ the control variable X. The force constant k is chosen to give the same spatial distribution to the adatom as the substrate atoms have, but the results are quite insensitive to the precise value of k.[3] The thermodynamic averaging selects the most favorable collective motion of the atoms.

Observing the work required to move X from one binding site to another, we can map out a free energy surface $A(X)$. Because of the three-body forces in the SW potential, it is not possible to specify a priori over what path the adatom should be dragged. So, we actually replace $X \rightarrow \mathbf{R}$ and observe both the force associated with moving $\mathbf{R}$ and the curvature tensor associated with $A(\mathbf{R})$ so that we can discover the sequence of configurations that would be associated with a reaction coordinate.

There is always an external field that will make an improbable configuration into an equilibrium configuration whose free energy can be determined. The second new feature of the hopping problem is that there are two contributions to $A(\mathbf{R})$, a contribution from the force associated with the change of density of states and a contribution from the force an external apparatus exerts to create $U(\mathbf{r})$. As we are only interested in the density of states contribution, we must disentangle these. This requires observing two properties along a reaction path. For each $\mathbf{R}$, we observe both the conjugate force and $\langle \mathbf{r} \rangle$.[3]

The analogous problem for a simple mechanical system would be trying to determine a potential $V(\mathbf{r})$ in a system whose natural motion is to find the minimum in $V(\mathbf{r})$ by exerting an external force on the system. If we add an external field, $V(\mathbf{r}) \rightarrow V(\mathbf{r}) + U_{\mathbf{R}}(\mathbf{r}) = \boldsymbol{V}(\mathbf{r}) + (1/2)k(\mathbf{r} - \mathbf{R})^2$, the minimum is now fixed by

$$\mathbf{F}_{\mathbf{R}} = -k(\mathbf{r} - \mathbf{R}) = \nabla V(\mathbf{r}) \tag{31}$$

by the balance between the external force $-k(\mathbf{r} - \mathbf{R})$ and the system's force $-\nabla V(\mathbf{r})$. To reconstruct $V(\mathbf{r})$, we prescribe $\mathbf{R}$ and observe both $\mathbf{r}$ and $\mathbf{F}_{\mathbf{R}}$. By taking $\mathbf{r}$ as independent, $\mathbf{R} = \mathbf{R}(\mathbf{r})$, and integrating $\nabla V(\mathbf{r})$ with respect to $\mathbf{r}$ gives $V(\mathbf{r})$.

The optimal positioning of $U(\mathbf{r})$ was determined for the three hops shown in Figure 9. From observations of the work required

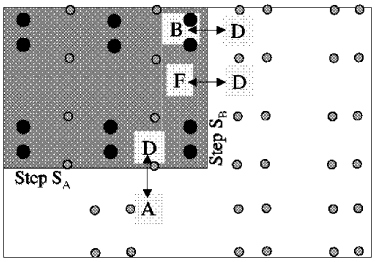

Figure 9. A, B, D, and F label binding sites on 2×1 surfaces. The shading pattern of Figure 1 is used to indicate the height of atoms (the shaded rectangle in the upper left corner is one layer higher than the nonshaded area). Both S_A and S_B steps are present. The double-headed arrows mark the hops for which the activation free energy was determined.

TABLE 3: Sample Size Dependence of the Surface Free Energy

surface size	γ (SW units)	thickness
6×6	0.565/atom	12 layers
4×12	0.554/atom	12 layers

TABLE 4: Rates of Hopping over Steps

step	sites connected	rate
S_A	D → A	$1.0 \cdot 10^{-3} \exp(-0.4\ \text{eV}/k_BT)$
S_B	B → D	$1.1 \cdot 10^{-3} \exp(-0.52\ \text{eV}/k_BT)$
S_B	F → D	$1.4 \cdot 10^{-3} \exp(-0.70\ \text{eV}/k_BT)$

to move $U(\mathbf{r})$ along the optimal path, we constructed $A(\mathbf{R})$ functions. The contributions from the density of states and the coupling to an external field were separated by observing the displacement between the location of $U(\mathbf{r})$ and the location of the adatom. The rates in Table 4 are given in an Arrhenius form in which the exponentials represent the activation free energies found in the simulations. There is considerable uncertainty in finding the optimum reaction path from a discrete set of observations, and each path represents a distinct problem. For this reason, the activation energies are no more accurate than the significant figures given in Table 4. The preexponential factors in Table 4 are $\sqrt{\kappa/m}/2\pi$ with κ the curvature of the free energy surface at the binding sites (fairly accurately known) and m the mass of the adatom (a very rough approximation)[35]. The rates of hopping over a step differ little from the corresponding rates of hopping between the same sites in the absence of a step.[3]

VII. Discussion

To predict which silicon surface reconstructions are realized in practice, one needs to know the free energy at the temperature of interest of the different reconstructions. While surface energy calculations[2,5,6,36−40] (0 K) provide some guide, it is the surface free energies that are strictly required to compare different reconstructions. Our calculations provide a first look at the effect of temperature on the relative stability of reconstructions.

The methods we have presented for determining the surface and line free energies are exact in the sense that they realize the formal definitions of these quantities. They give accurate results, because the structural change on our simulation paths is minimal. It is only this feature that distinguishes our method from earlier simulations of interfacial free energies. The pioneering work of Broughton and Gilmer[41,42] used a simulation path that varied T over a significant range and looked for differences in properties associated with large structural changes. We have been guided by the recognition that the noise on a simulation path increases when there is a large structural change on the path.[16] The first paths proposed sought to determine the work required to physically split a perfect crystal. This is a very irreversible process in practice, and constructing a reversible analogue required considerable experimentation and some minor modifications of the interaction potentials. To avoid this experimentation, Snook et al.[43] introduced a more clearly reversible path to split a crystal: A purely repulsive potential is introduced across a crystal plane. This is still an image of a laboratory path, however, involving unnecessary structural changes.

Our path, by contrast, creates two free surfaces (in Step 1) with no first-order change in structure at all. The path is short, and the conjugate force is not a noisy observable, so an accurate free energy change is easily determined. In the subsequent steps (selecting the targeted reconstruction and then relaxing the surface structure), the structural changes in the system are again minimal. As the fluctuations in the conjugate forces along the paths of these steps remain small, all intermediate states are quite metastable. But the targeted reconstructions are, of course, only metastable. The objective from the outset was to determine the free energy of metastable states.

The practical realization of our method does involve two approximations. First, we have assumed that the silicon crystals can be described as a classical system with forces derived from the SW interaction potential. Strictly speaking, our results describe the properties of the SW model. While this potential describes the Si(100) surface rather well, the description is not perfect. The most discussed defect of the SW potential (or any semiempirical potential for silicon) is the prediction of symmetric dimer structures. Low-temperature observations[7−9] show buckled dimers (the two atoms of dimers are at different heights). This tilting of dimer bonds leads to local $p(2 \times 2)$[7,44] and $c(2 \times 4)$[10] reconstructions at low temperatures. But buckling is only seen at temperatures $T \approx 80-200$ K, and STM experiments report symmetric dimers at and above room temperatures. Quantum calculations[36] similarly identify buckled ground-state structures, but the reported energy differences between $p(2 \times 1)$, $p(2 \times 2)$, and $c(2 \times 4)$ structures are rather small. (The energy lowering of the buckled dimer with respect to a symmetric dimer is $\sim 0.12-0.2$ eV/dimer, which is much less than the energy lowering due to basic dimerization ~ 2 eV/dimer.) Stillinger[45] has shown that the SW potential can be fine-tuned to show buckled dimers, but there is a metastable configuration with slightly higher energy that has all of the dimers parallel. MD simulations[46] with this potential suggest that there is a first-order phase transition (at a temperature $T \approx 200$ K) between a thermodynamic state with tipped dimers and a state with parallel dimers. At the temperature $T = 1000$ K of our simulations, $k_BT = 0.09$ eV. This most obvious structural defect of the potential is probably irrelevant in our simulations. Other more subtle errors are harder to assess, however.

The second approximation is associated with the fact that we simulate fairly small systems. Finite size effects are important. To estimate the magnitude of finite size effects on the surface free energy calculations, we simulated two different surface sizes. The results given in Table 3 give an estimate of the finite size effect errors.

The line free energies are, in fact, differences between numbers that are proportional to the size of the surface. As our surfaces are not that large, the difference is significant, but this comes at the price of being far from the thermodynamic limit for the β's. This is to be contrasted with determinations of line free energies at finite temperatures[23,24] by fitting experimental

data such as kink distributions to surface structure models with empirical potentials.

We have simulated linear steps. The inclusion of nonlinear configurations in S_B steps introduces S_A-like segments of the edge that are associated with very low free energy increments.[19,32,47] This explains the observed wavy structure of S_B steps and suggests that a capillary wave renormalization of our line free energies should be made.

Mesoscopic studies of Alerhand[28,32] suggest that there are contributions to the line free energy that go as the logarithm of the distance to the next step, making the planar (100) surface unstable toward the spontaneous formation of a stepped surface. Some verification of this picture has been provided by computations of Poon[39] and Schofield[38] (using classical potentials in large systems) that show that there are large finite size effects for the line free energy and by experimental observations of Zhong et al.[18] If there is truly a logarithmic contribution at $T > 0$, then the Gibbs subtractive definition given in eq 20 will not describe reality. While we do see changes in the line free energies when we increase the size of our system, we did not examine large enough systems to test this suggestion.

Acknowledgment. S.S. and B.K. would like to thank the epitaxial division of MEMC Electronic Materials Inc., St. Peters, MO, for partial financial support of this work. R.L. would like to acknowledge the U.S. National Science Foundation (CHE-9529327) for partial support.

References and Notes

(1) Stillinger, F. H.; Weber, T. A. *Phys. Rev. B* **1985**, *31*, 5262.
(2) Balamane, H.; Halicioglu, T.; Tiller, W. A. *Phys. Rev. B* **1992**, *46*, 2250.
(3) Somasi, S.; Khomami, B.; Lovett, R. *J. Chem. Phys.* **2003**, *119*, 9783.
(4) Schlier, R. E.; Farnsworth, H. E. *J. Chem. Phys.* **1959**, *30*, 917.
(5) Khor, K.; Sharma, S. *Phys. Rev. B* **1987**, *36*, 7733.
(6) Weber, T. *Mater. Res. Soc. Symp. Proc.* **1985**, *63*, 162.
(7) Tromp, R. M.; Hamers, R. J.; Demuth, J. E. *Phys. Rev. Lett.* **1985**, *55*, 1303.
(8) Hamers, R. J.; Tromp, R. M.; Demuth, J. E. *Phys. Rev. B* **1986**, *34*, 5343.
(9) Jayaram, G.; Xu, P.; Marks, L. D. *Phys. Rev. Lett.* **1993**, *71*, 3489.
(10) Enta, Y.; Suzuki, S.; Kono, S. *Phys. Rev. Lett.* **1990**, *65*, 2704.
(11) Lin, D.-S.; Wu, P.-H. *Surf. Sci.* **1998**, *397*, L273.
(12) Uhrberg, R.; Northrup, J.; Biegelsen, D.; Bringans, R.; Swartz, L.-E. *Phys. Rev. B* **1992**, *46*, 10251.
(13) Somasi, S.; Khomami, B.; Lovett, R. *J. Chem. Phys.* **2000**, *113*, 4320.
(14) Nosé, S. In *Computer Simulation in Materials Science*; Meyer, M., Pontikis, V., Eds.; Kluwer: Dordrecht, 1991.
(15) Somasi, S.; Khomami, B.; Lovett, R. *J. Chem. Phys.* **2001**, *114*, 6315.
(16) Sheu, S.-Y.; Mou, C.-Y.; Lovett, R. *Phys. Rev. E* **1995**, *51*, R3795.
(17) Griffith, J.; Kochanski, G.; Kubby, J.; Wierenga, P. *J. Vac. Sci. Technol., A* **1989**, *7*, 1914.
(18) Zhong, L.; Hojo, A.; Matsushita, Y.; Aiba, Y.; Hayashi, K.; Takeda, R.; Shirai, H.; Saito, H.; Matsushita, J.; Yoshikawa, J. *Phys. Rev. B* **1996**, *54*, R2304.
(19) Swartzentruber, B.; Mo, Y.-W.; Webb, M.; Lagally, M. *J. Vac. Sci. Technol., A* **1989**, *7*, 2901.
(20) Swartzentruber, B.; Kitamura, N.; Lagally, M.; Webb, M. *Phys. Rev. B* **1993**, *47*, 13432.
(21) Tromp, R.; Reuter, M. *Phys. Rev. B* **1993**, *47*, 7598.
(22) Tromp, R.; Reuter, M. *Phys. Rev. Lett.* **1992**, *68*, 820.
(23) Zandvliet, H.; Elswijk, H.; van Loenen, E.; Dijkkamp, D. *Phys. Rev. B* **1992**, *45*, 5965.
(24) Zandvliet, H.; van Dijken, S.; Poelsema, B. *Phys. Rev. B* **1996**, *53*, 15429.
(25) Yang, H. Q.; Zhu, C.; Gao, J.; Xue, Z.; Pang, S. J. *Surf.Sci.* **1999**, *429*, L481.
(26) Wierenga, P.; Kubby, J.; Griffith, J. *Phys. Rev. Lett.* **1987**, *59*, 2169.
(27) Zandvliet, H.; Elswijk, H. *Phys. Rev. B* **1993**, *48*, 14269.
(28) Alerhand, O. L.; Vanderbilt, D.; Meade, R. D.; Joannopoulos, J. D. *Phys. Rev. Lett.* **1988**, *24*, 1973.
(29) Aspnes, D. E.; Ihm, J. *J. Vac. Sci. Technol., B* **1987**, *5*, 939.
(30) Aspnes, D. E.; Ihm, J. *Phys. Rev. Lett.* **1986**, *57*, 3054.
(31) Mukherjee, S.; Pehlke, E.; Tersoff, J. *Phys. Rev. B* **1994**, *49*, 1919.
(32) Alerhand, O.; Berker, A. N.; Joannopoulos, J.; Vanderbilt, D. *Phys. Rev. Lett.* **1990**, *64*, 2406.
(33) Chadi, D. *Phys. Rev. Lett.* **1987**, *59*, 1691.
(34) Dyson, A.; Smith, P. *Mol. Phys.* **1999**, *96*, 1491.
(35) Skinner, J. L.; Wolynes, P. G. *J. Chem. Phys.* **1980**, *72*, 4913.
(36) Ramstad, A.; Brocks, G.; Kelly, P. *Phys. Rev. B* **1995**, *51*, 14504.
(37) Zhu, Z.; Shima, N.; Tsukada, M. *Phys. Rev. B* **1989**, *40*, 11868.
(38) Schofield, S.; Radny, M.; Smith, P. *Phys. Rev. B* **2000**, *62*, 10199.
(39) Poon, T. W.; Yip, S.; Ho, P. S.; Abraham, F. F. *Phys. Rev. Lett.* **1990**, *65*, 2161.
(40) Abraham, F.; Batra, I. *Surf. Sci. Lett.* **1985**, *163*, L752.
(41) Broughton, J. Q.; Gilmer, G. H. *J. Chem. Phys.* **1983**, *79*, 5095.
(42) Broughton, J. Q.; Gilmer, G. H. *J. Chem. Phys.* **1986**, *84*, 5741.
(43) Grochola, G.; Russo, S. P.; Snook, I. K.; Yarovsky, I. *J. Chem. Phys.* **2002**, *117*, 7685.
(44) Wolkow, R. A. *Phys. Rev. Lett.* **1992**, *68*, 2636.
(45) Stillinger, F. H. *Phys. Rev. B* **1992**, *46*, 9590.
(46) Stillinger, D. K.; Stillinger, F. H. *Phys. Rev. B* **1993**, *48*, 15047.
(47) Hoven, A. J.; Lenssinck, J. M.; Dijkkamp, D.; van Loenen, E. J.; Dieleman, J. *Phys. Rev. Lett.* **1989**, *65*, 1830.